21

White Light Sensing Systems for High Voltage Measuring Using Electro-Optical Modulators as Sensor and Recovery Interferometers

Josemir C. Santos[1], José C. J. Almeida[2] and Luiz P. C. Silva[1]
[1]*University of São Paulo*
[2]*Optsensys*
Brazil

1. Introduction

There are several known issues related to the use of electro-optical sensors as measuring devices. In applications intended for use in measuring currents and potentials in high voltage electric power systems, optical sensor systems must attend severe specifications, such as: large withstand voltage of the primary sensor, high accuracy (better than 0,5%, in case of revenue metering), long term stability of scale factor, large dynamic range (>50 dB, in some applications for protection purpose) and relatively wide frequency response range (of several kHz, in case that harmonics content evaluation is needed). However, the potential advantages arising from the use of optical fiber sensors as instrument transformers (ITs) in substitution to conventional electromagnetic transformers, may explain the intensive efforts that have been done during the last 30 years to develop optical ITs.

In a previous work (Santos, 2009), focused on the development of electro-optical sensors applied to direct measuring high voltages, in order to fulfill the requirements for ITs previously described, various sensing systems linked by optical fibers were presented. The progress in this field is commonly divided into three main approaches.

In the first approach, conventional transformers connected to primary electronic converters and communicated by means of optical fiber links to secondary converters have been used to improve the EMI toughness and to provide complete electrical isolation between the measured and the measuring systems. Typical examples of such approach (Crotti et al., 2006; Rahmatian, 2010) describe conventional ITs connected to primary electronic converters that generate modulated optical signals and provide their adequate coupling to optical fiber communication links.

In the second aproach, non-conventional transformers, also called as electronic transformers, have been developed using different types of sensors or transducers as measuring devices that are connected by optical fiber links to secondary converters. In representative examples of this approach (Bull et al., 2005; Mariscotti, 2009) Rogowski coils are used as sensor element.

The third approach consists in using optical sensors to directly measuring of voltage or current in high voltage systems. Passive optical sensors, such as electro-optical and

magneto-optical modulators, are attractive for such purpose because all their components can be made with dielectric materials and have small dimensions. Since these sensors, generally, show low sensitivity to EMI and wide frequency response, they usually have much superior performance characteristics than the conventional transformers, and are capable to make better use of potentially excellent quality of the optical fiber links.

The linear electro-optic effect, also called Pockels effect, has been largely used to build electro-optical modulators that have many applications in communications, signal processing and sensing systems. These modulators can be used as sensors for measuring of electric field, current and voltage, among other quantities. The optical sensors used as ITs for measuring voltage and current are called Optical Voltage Transformers (OVTs) and Optical Current Transformers (OCTs), respectively.

The main problem in trying to apply electro-optical sensors to perform direct measuring of potentials at high voltage levels is their sensitivity to applied voltage, commonly too high in comparison with the voltage to be measured. Since in typical Pockels modulators the transmitted light intensity has a sinusoidal dependency with applied modulation voltage, as shown later in this chapter, there is a limit for holding a univoque relationship between the transmitted light intensity and the applied voltage, imposing a restriction in maximum value of applied voltage that can be actually measured.

A solution that has been adopted to allow measuring of higher voltages relies in using capacitive or resistive potential dividers for obtaining a sample of the high voltage to be measured and to apply this low voltage signal to the optical sensor. This solution limits the performance of the OVT to that of the potential divider, which is not always satisfactory. The most favorable solution, however, should be the direct application of high voltages to a properly designed Pockels modulator, avoiding the use of dividers and, therefore, making the best use of superior characteristics of optical sensors. To reach this goal, the Pockels modulator should be built in an appropriate configuration, in order to increase its dielectric withstand and reduce its sensitivity to suitable values. Several alternatives have been proposed to build optical fiber sensors appropriate for high voltage measuring systems, but a small number of them could lead to practical devices able to be used in field applications.

Another approach to solve the posed problem is the application of a different interrogation technique, instead of the polarimetric intensity modulation normally used in Pockels modulators, capable to extend the dynamic range of the sensor to a sufficiently high value.

Recently, the White Light Interferometry (WLI) technique has been used as an alternative to implement optical fiber sensor systems that can meet severe specifications, similar to the requirements of applications as in ITs. White light interferometric systems based on interferometers linked by optical fibers have been largely used for implementation of various high performance optical sensors on trial basis. The design of a specific sensor depends upon the particular requirements of its application as well as the physical quantity to be measured, which may be, for example, displacement, strain, temperature, etc. In such a kind of WLI sensor systems, a broadband light source is used to illuminate two interferometers that are connected in series by an optical fiber link. The application of this method can add a large dynamic range to the high accuracy, which is a typical advantageous characteristic of conventional interferometric sensor systems.

Following this approach, it is shown in this chapter how WLI technique can be applied to a Pockels voltage sensor, enhancing its performance while keeping its linearity and accuracy.

At first, the general concepts related to WLI are presented.

Next, it is introduced an application, originally proposed by the first author, in which the WLI is used together with two electro-optical modulators, based on the Pockels effect, for measuring high voltages directly. Since this approach has no moving parts, the frequency bandwidth achievable can be much higher than any mechanically or electronically scanned WLI system previously proposed.

Finally, practical realizations of ITs based on WLI sensor systems using electro-optical modulators as sensor and recovery interferometers are presented. Special attention is given to electronic signal processing techniques used to demodulate the optical signal available at the output of the sensor system. Two different techniques are depicted; both capable to perform measuring with compensation for fluctuations on optical average power delivered at the output of sensor system. Such fluctuations normally arise from variations in attenuations or variations in the output power of optical source, for example. Experimental investigations carried out with the sensor systems developed are presented, including experimental results obtained with both electronic signal processing techniques. At the end of chapter, a brief discussion on the future perspectives and under developing initiatives related to this field is addressed.

2. Principles of White Light Interferometry (WLI) sensing

In typical interferometric optical sensors, highly monochromatic (or long coherence length) light sources are commonly used, therefore the unambiguous measurement range is limited to one period of the interferometer transfer function and the basic unit of measurement is the source wavelength.

By the other hand, white light interferometry has, potentially, the capability of identifying the interference fringe order from the output fringe pattern by using a broadband optical source (Chen, 1992). As a result, the unambiguous range of the output signal is no longer limited to within half of a fringe, and an absolute phase measurement over a large operating range can be achieved. The output intensity pattern of a white light interferometer has a visibility profile determined by the low-coherence property of the broadband source used.

Since the output of an interferometer is, in theory, the Fourier transform of the source spectrum (Françon, 1967) and the Fourier transform a Gaussian function is also a Gaussian function, it follows that the normalized output intensity pattern of a white light interferometer is a cosine function modified by a Gaussian visibility profile, as shown in Fig. 1. This output intensity pattern is commonly also called as fringe pattern in optical engineering field.

The principle of WLI sensing may be explained by using Fig. 2, which shows a block diagram of a generic WLI sensor system.

In Fig. 2 it is shown that light emitted from a spectrally broadband source, for example a superluminescent diode (SLD), is coupled via a beam splitter into an optical fiber link connected to the sensor interferometer. The optical path difference (OPD) introduced by the

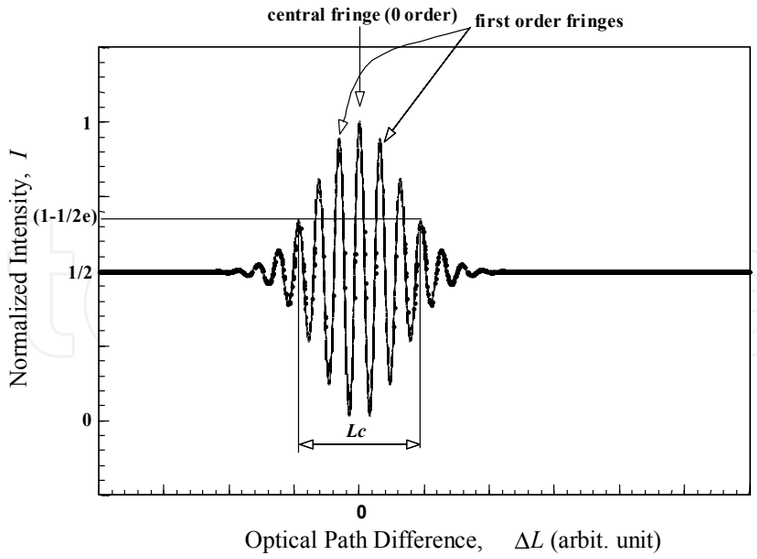

Fig. 1. Theoretical output intensity pattern of a white light interferometer.

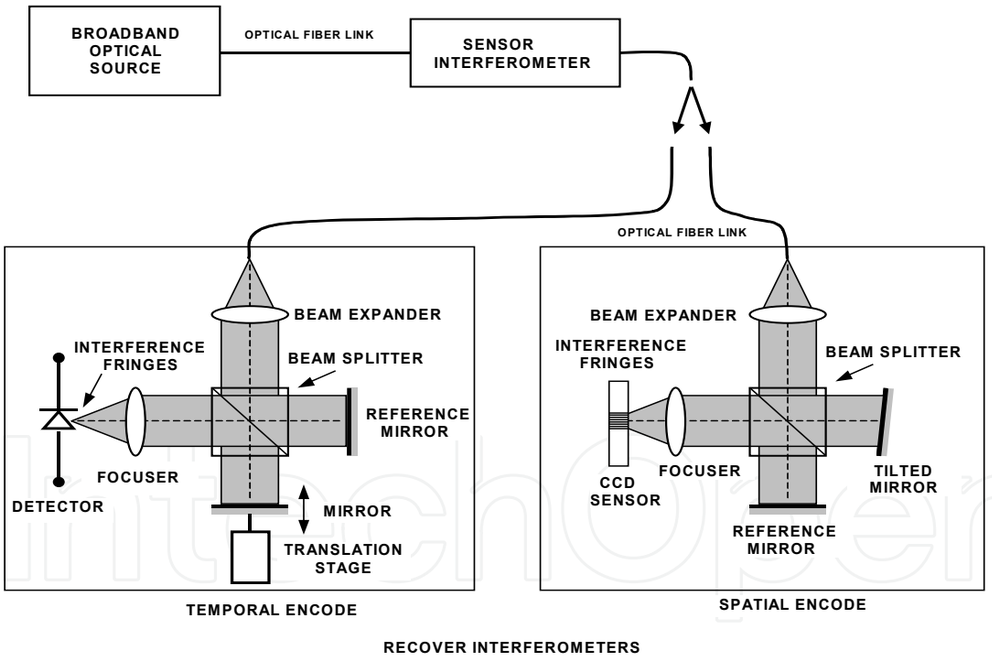

Fig. 2. Principle of operation of a white light interferometric sensor.

sensor interferometer, $\Delta L_s(X)$, is linearly sensitive to the external measurand X. If the OPD introduced by the sensing interferometer is greater than the coherence length of the source, L_c, no interference is observed at the output light of the sensor interferometer. When the output of sensor interferometer is linked to the input of a second interferometer, called as "recovery" interferometer, scanning of the path difference introduced by this interferometer, $\Delta L_r(Y)$, results in interference being observed at its output when $\Delta L_r(Y)$ approaches to $\Delta L_s(X)$.

Neglecting the spectral dependency of OPD, the behavior of light intensity at the output of sensor interferometer, I_s, as a function of light wavenumber, σ, can be described by the following relation (Lequine, 1990):

$$I_s(\sigma) = T_1 T_s I_o(\sigma)\left\{1 \pm K_s \cos\left[2\pi\sigma\Delta L_s(X)\right]\right\} \tag{1}$$

where T_1 is the transmission factor of the forward fiber link, T_s and K_s are the transmission factor and the visibility of sensor interferometer, respectively, and $I_0(\sigma)$ is the spectral intensity distribution of the light source. Analogously, the behavior of the recovery interferometer can be written as:

$$I_r(\sigma) = T_2 T_r I_s(\sigma)\left\{1 \pm K_r \cos\left[2\pi\sigma\Delta L_r(Y)\right]\right\} \tag{2}$$

where T_2 is the transmission factor of return fiber link and T_r and K_r are the transmission factor and the visibility of recovery interferometer, respectively. The OPD introduced by the recovery interferometer, $\Delta L_r(Y)$, is linearly sensitive to scanning quantity Y. The total intensity available for detection at the output of WLI system is calculated by integrating the previous equation over all the wavenumbers, and, if the source has a Gaussian spectral distribution, this integral becomes:

$$I = T_1 T_2 T_s T_r I_0 \left\{1 + K_{0s} K_{0r} e^{-\left[\pi\frac{(\Delta L_s - \Delta L_r)}{L_c}\right]^2} \cos\left[2\pi\frac{(\Delta L_s - \Delta L_r)}{\lambda_0}\right]\right\} \tag{3}$$

The resulting intensity signal, I, appears in eq. (3) as a cosine function modified by a visibility function, both dependent of the OPD difference, exactly as shown in Fig. 1. Both eq. (3) and Fig. 1 show that, at the matching point, the interferometer output is at the center of the brightest fringe. The order of this fringe is zero and it is called *central fringe*. The fringe-order identification is dependent on the identification of central fringe.

To achieve a precise measurement in a large dynamic range, the sensor system must, at first, correctly identify the central fringe and then measure accurately the OPD introduced by the recovery interferometer, $\Delta L_r(Y)$, necessary to lead the system to the matching point, i.e., the center of central fringe. There are several proposed methods to reach this aim, using different topologies and signal processing techniques. The two most commonly used OPD scanning techniques, the temporal encode and the spatial encode, are illustrated in Fig. 2.

Temporal encode techniques make use of mechanically tunable OPD interferometers to scan the fringe pattern and record it for further analysis. This method allows high accuracy and low signal-to-noise ratio (SNR) level, but it is normally very slow, since it uses moving parts.

In a system using electronically scanned (spatial encode) WLI, the interference fringes pattern is produced by superposing two expanded light beams. The resulting pattern is imaged over a CCD array. This method is much faster than the temporal encoding, but the fringe visibility is reduced due to spatial coherence mismatches and intrinsic noises of beam profile and CCD array (Ning et al., 1995).

In both cases, the signal processing techniques normally include digital treatment of the signal and the computation time may limit the response frequency bandwidth of the sensor system. Besides these two techniques, other electronically scanned methods using dual wavelength light sources and no moving parts can be applied to WLI sensors.

In this chapter a new approach for temporal encoded WLI sensor systems with no moving parts is proposed by using a Pockels electro-optic modulator as recovery interferometer. In such approach, the frequency bandwidth of the system can be significantly enhanced while keeping a large measuring range of operation.

3. WLI method applied to fiber optical linked electro-optical sensor systems

Recently, several WLI sensor systems have been proposed to measure different physical quantities (measurands). In Table 1 some examples are listed and information are given about the measurand, the encoding technique, the bandwidth and the dynamic range for each sensor.

Measurand	Encoding Technique	Bandwidth	Dynamic Range	Reference
Temperature	Temporal (fiber stretch)	30 Hz	20 ~ 70 ^{o}C	(Kim, 2008)
Position	Temporal (moving mirror)	< 1 Hz	0 ~ 7.2 mm	(Chen, 2010)
Displacement	Temporal (moving mirror)	~20 Hz	0 ~ 1050 nm	(Liao, 2010)
Micro-Strain	Temporal (moving lens)	1 Hz	0 ~ 350 με	(Velosa, 2011)
Temperature	Temporal (moving lens)	> 60 Hz	35 ~ 75 ^{o}C	(Yu, 2005)
Displacement	Spatial (electronically scanned)	~500 Hz	0 ~ 20 μm	(Murtaza, 1991)

Table 1. Examples of WLI sensor systems

From table 1, it is possible to observe that typical WLI sensor systems presented show dynamic ranges that can be considered larges, when compared with the ones achievable by normal interferometric systems in same conditions. However, in all cases, relatively narrow bandwidths are observed, preventing the use of mentioned systems in applications intended for measurement of fast varying measurands.

In alternate current (ac) electrical power systems the main electrical measurands of interest are voltage and current, and the lowest nominal frequency of these quantities is 50 Hz. Therefore, only the example shown in last line of table 1 could be applied to measure such quantities with significant information about their harmonic content. Furthermore, larger bandwidth may be required from a sensor system to be applicable as IT for protection purposes, since they must to respond to transitory phenomena, such as short circuits or lightning and switching impulses, which superpose overvoltage and overcurrent variations much faster than the period associated to the nominal frequency. Consequently, practical application of WLI technique in optical ITs demands advances in the fields of encoding techniques and signal processing schemes, to allow production of sensor systems able to provide bandwidths sufficiently larges to attend requirements of defined accuracy classes, which will depend on the foreseen use of IT for metering or protection.

Recently a new encoding technique based on electro-optical interferometers has been developed to overcome both mentioned limitations, in dynamic range and bandwidth, for the specific case of OVT to be used for measuring in high voltage electric power systems.

Most part of electro-optical sensors utilized in OVTs makes use of electro-optic modulators based on Pockels effect configured as birefringence interferometers. In this case, there is a limitation in dynamic range of measured voltage, which is a typical disadvantage arising from the polarimetric method used for measuring the electrically induced phase retardation due to the Pockels effect, since normal interferometric methods are useful only to measure OPD in the range of one wavelength. However, as described earlier, WLI sensor systems are based on interferometers linked in series by optical fibers. Therefore, by linking in series two properly designed Pockels modulators configured as birefringence interferometers, one as voltage sensor and other as recovery interferometer, it is possible to set up a WLI sensor system.

The working principle of a Pockels modulator, represented as shown in Fig. 3, can be described as a two-beam birefringence interferometer by assuming that the components of incident light, which are polarized parallel to x and y axes, are two independent beams having intensities I_x and I_y, respectively. When light is crossing the Pockels crystal, both components travel along a path of same length, L, which is the length of crystal, but each one is affected by a different refractive index. The difference between these two refractive indices, $\Delta n = n_y - n_x$, is the birefringence of medium. The light emerging from the crystal crosses a second polarizer, called as analyzer, which is oriented at 45° with respect to

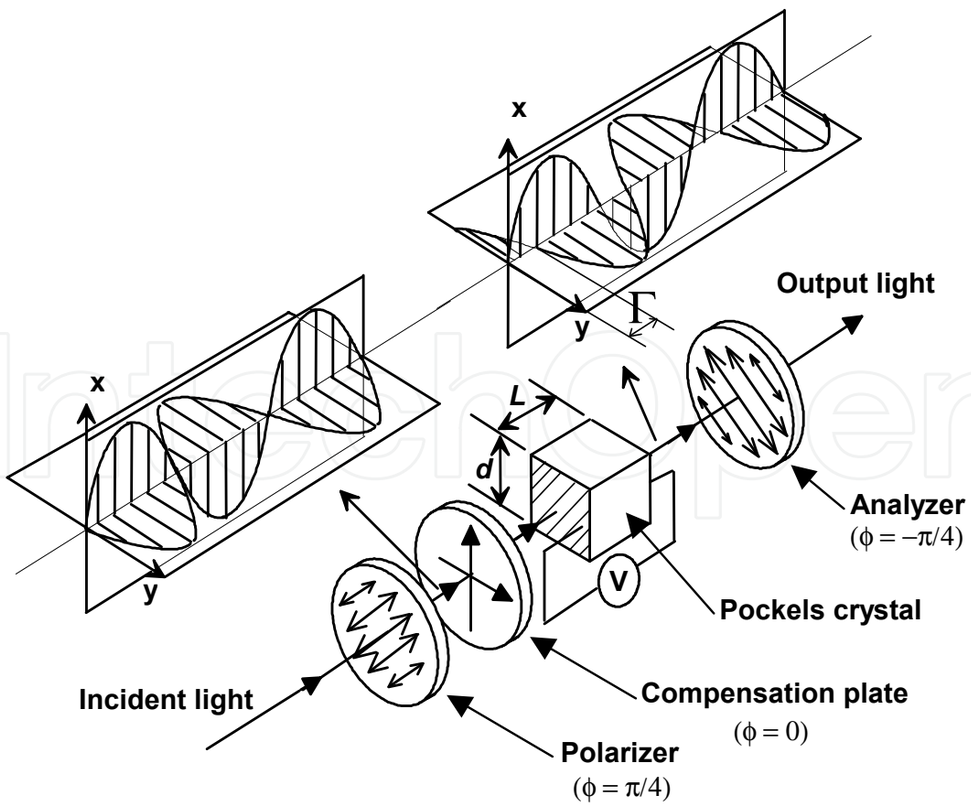

Fig. 3. Pockels sensor regarded as a two-beam birefringence interferometer.

polarization directions of both components. Since the analyzer transmits only the part of light intensity of each component that is parallel to its polarization direction, interference of the two light components occurs at its output.

The key part in designing a Pockels modulator is the calculus of its birefringence. The general procedure involved in this task depends on several parameters, such as: the specific crystal selected (including its optical and electrical characteristics, geometry and dimensions), the configuration chosen (longitudinal or transverse) and the relative orientation among the propagation direction, the electric filed direction and the crystal's optical axes directions.

For example, using an electro-optical crystal with cubic lattice (of $\bar{4}3m$ symmetry group, for instance), in a polarimetric modulator in longitudinal configuration as shown in Fig. 3, where polarizer and analyzer polarization directions are crossed to each other, the propagation direction is parallel to an optical axis of crystal, and considering that applied voltage V generates an uniformly distributed electric field, E, inside crystal, which implies that $E = V/L$, the electricaly induced birefringence, Δn_e, becomes (Yariv & Yeh, 1984):

$$\Delta n_e(V) = n_o^3 r_{41} E = n_o^3 r_{41} \frac{V}{L} \tag{4}$$

where n_O is the ordinary refractive index and r_{41} is, in this case, the only relevant electro-optic coefficient of crystal.

The electrically induced phase retardation, Γ_e, between the two orthogonal light components is:

$$\Gamma_e = \frac{2\pi}{\lambda} \Delta n_e \times L \tag{5}$$

where λ is the wavelength of light inside crystal when there is no applied voltage.

In this case, the half-wave voltage, which is defined as the value of V that makes $\Gamma_e = \pi$, is given by (Almeida, 2001):

$$V_\pi = \frac{\lambda}{2 n_o^3 r_{41}} \tag{6}$$

The total phase retardation, Γ_t, is the summation of the electrically induced phase retardation, Γ_e, with a fixed contribution of compensation plate, $\Delta\phi_c$, and can be written as:

$$\Gamma_t = \Delta\phi_c + \frac{2\pi}{\lambda} \Delta n_e \times L = \Delta\phi_c + \frac{2\pi}{\lambda} n_o^3 r_{41} V \tag{7}$$

The total optical phase retardation can be also given in terms of V_π by:

$$\Gamma_t = \Delta\phi_c + \pi \frac{V}{V_\pi} \tag{8}$$

By using eq. (8) the optical path difference, ΔL, correspondent to this optical phase retardation is given by:

$$\Delta L = \frac{\lambda}{2\pi}\Gamma_t \tag{9}$$

Applying eq. (7) to this relation, the total path difference becomes

$$\Delta L = \Delta L_c + n_o^3 r_{41} V \tag{10}$$

where $\Delta L_c = \frac{\lambda}{2\pi}\Delta\phi_c$ is the OPD introduced by the compensation plate.

From eq. (10), it is found that the total OPD in this interferometer is independent of wavelength and is linearly dependent on applied voltage. Since the two beams have crossed polarization directions they cannot interfere with other. The recombination of beams is made by the analyzer, which actually is a polarizer with its polarization direction oriented at -45º with respect to *x* axis. Since these two beams have the same intensity ($I_x = I_y$) and only half of intensity of each beam is transmitted by the analyzer, the visibility of its central fringe is $K_{0s} = 1$, and the transmission factor of this sensing interferometer is:

$$T_s = \frac{1}{2}\alpha_s \tag{11}$$

where α_s is the attenuation introduced in the transmitted light by the sensing interferometer due to factors such as reflections, scattering, misalignments, absorption, etc.

The behavior of this interferometer is given, from eq. (2), by:

$$I_s(\sigma) = T_1\,\alpha_s\,\frac{1}{2}I_o(\sigma)\left\{1 \pm \cos\left[2\pi\sigma\left(\Delta L_c + n_o^3 r_{41} V\right)\right]\right\} \tag{12}$$

If a second Pockels birefringence interferometer is linked in series with the sensing interferometer described above, the overall behavior of the white light interferometric sensor system obtained is given, analogously to eq. (3), by:

$$I = \frac{1}{4}\alpha_s\alpha_r\,T_1T_2\,I_0\left\{1+\frac{1}{2}e^{-\left\{\left[(\Delta L_{cs}-\Delta L_{cr})+n_o^3 r_{41}(V_s-V_r)\right]\frac{\pi}{L_c}\right\}^2}\cos\left[2\pi\frac{(\Delta L_{cs}-\Delta L_{cr})+n_o^3 r_{41}(V_s-V_r)}{\lambda_0}\right]\right\} \tag{13}$$

where indices *s* and *r* correspond to values related to sensor and recovery interferometer, respectively, and L_c is the coherence length of source, given by (Yu, 2005):

$$L_c \cong \frac{\lambda_0^2}{d\lambda} \tag{14}$$

where λ_0 is the central wavelength of low-coherence source in vacuum and $d\lambda$ is the spectral width of source.

In order to operate the sensor system near to central fringe, both OPDs introduced by retardation plates must to be equal. In this situation, $\Delta L_{cs} - \Delta L_{cr} = 0$ and eq. (13) becomes:

$$I = \frac{1}{4}\alpha_s \alpha_r T_1 T_2 I_0 \left\{ 1 + \frac{1}{2} e^{-\left\{ \left[n_o^3 r_{41} (V_s - V_r) \right] \frac{\pi}{L_c} \right\}^2} \cos\left[2\pi \frac{n_o^3 r_{41} (V_s - V_r)}{\lambda_0} \right] \right\} \tag{15}$$

It is found from last equation that, for a system built as described, the voltage applied to recovery interferometer, V_r, must to be equal to the voltage to be measured, V_s, in order to reach the maximum light intensity at system output. Therefore, by observing the output light intensity, I, meanwhile V_r is changed and measuring V_r when I is at maximum, it is possible to know directly the value of V_s at that moment.

The measuring method just described corresponds to a hybrid encoding technique, since it can be considered as temporal, once it could be necessary to scan periodically V_r to get one measured value of V_s per period and, also, it can be seem as electronically scanned, once there are no moving parts in the system and the OPD scanning is performed by means of an electro-optical device.

The exact classification of this technique, in fact, depends on how the electronic signal processing of the sensor system is implemented. The behavior and performance characteristics of the sensor system are ultimately defined by the association of encoding technique with the signal processing technique.

4. Application of WLI technique to a high voltage Pockels sensor system

Considering the application of a WLI sensor system as high voltage OVT, the method just described is not useful because it imposes the need to apply to recovery interferometer the same high voltage that is applied to the sensor interferometer, which is meaningless.

There are, at least, two possibilities for introducing a measurement scale factor in the sensor system, in order to reduce the maximum value of scanning voltage necessary to find the central fringe position. The first alternative consists of using different crystals in sensor and recovery interferometers. Choosing a crystal to be used in recovery interferometer with a product $n_{or}^3 r_{41r}$ greater than the product $n_{os}^3 r_{41s}$ of crystal used in sensor interferometer, the voltage V_r necessary to matches the OPD introduced by sensor interferometer will be smaller. In this case, eq. (15) becomes:

$$\begin{aligned} I &= \frac{1}{4}\alpha_s \alpha_r T_1 T_2 I_0 \left\{ 1 + \frac{1}{2} e^{-\left[\left(n_{os}^3 r_{41s} V_s - n_{or}^3 r_{41r} V_r \right) \frac{\pi}{L_c} \right]^2} \cos\left[2\pi \frac{n_{os}^3 r_{41s} V_s - n_{or}^3 r_{41r} V_r}{\lambda_0} \right] \right\} = \\ &= \frac{1}{4}\alpha_s \alpha_r T_1 T_2 I_0 \left\{ 1 + \frac{1}{2} e^{-\left\{ \left[n_{os}^3 r_{41s} (V_s - f V_r) \right] \frac{\pi}{L_c} \right\}^2} \cos\left[2\pi \frac{n_{os}^3 r_{41r} (V_s - f V_r)}{\lambda_0} \right] \right\} \end{aligned} \tag{16}$$

where $f = \dfrac{n_{or}^3 r_{41r}}{n_{os}^3 r_{41s}}$ is the scale factor.

The second alternative to introduce a scale factor is making use of a configuration in the Pockels modulator applied as sensor interferometer different than the configuration used in the modulator used as recovery interferometer. For example, a transverse modulation configuration can be applied in recovery interferometer while longitudinal modulation configuration is applied in sensor interferometer. In such a case, eq. (15) becomes:

$$I=\frac{1}{4}\alpha_s\alpha_r T_1T_2 I_0\left\{1+\frac{1}{2}e^{-\left\{\left[n_o^3 r_{41}\left(V_s-\frac{L}{d}V_r\right)\right]\frac{\pi}{L_c}\right\}^2}\cos\left[2\pi\frac{n_o^3 r_{41}\left(V_s-\frac{L}{d}V_r\right)}{\lambda_0}\right]\right\} \tag{17}$$

where d is the thickness of Pockels crystal used in the recovery interferometer and the scale factor is L/d. In order to describe in a general form the scale factor arising from the use of different electro-optic modulators in WLI sensor systems, eq. (15) may be represented in terms of V_π as follows:

$$\begin{aligned} I&=\frac{1}{4}\alpha_s\alpha_r T_1T_2 I_0\left\{1+\frac{1}{2}e^{-\left[\left(\frac{\lambda_0}{2V_{\pi s}}V_s-\frac{\lambda_0}{2V_{\pi r}}V_r\right)\frac{\pi}{L_c}\right]^2}\cos\left[\pi\left(\frac{1}{V_{\pi s}}V_s-\frac{1}{V_{\pi r}}V_r\right)\right]\right\}= \\ &=\frac{1}{4}\alpha_s\alpha_r T_1T_2 I_0\left\{1+\frac{1}{2}e^{-\left\{\left[\frac{\lambda_0}{2L_c}\frac{\pi}{V_{\pi s}}(V_s-f_\pi V_r)\right]\right\}^2}\cos\left[\frac{\pi}{V_{\pi s}}(V_s-f_\pi V_r)\right]\right\} \end{aligned} \tag{18}$$

where $V_{\pi r}$ and $V_{\pi s}$ are half wave voltages of Pockles modulators used as sensor and recovery interferometers, respectively, and the scale factor, expressed in terms of V_π, is: $f_\pi=\frac{V_{\pi s}}{V_{\pi r}}$.

The advantage in using f_π is that, regardless of all characteristics of any specific electro-optical modulator selected to be used as sensor or recovery interferometer, it is enough to calculate $V_{\pi r}$ and $V_{\pi s}$ to determine the optical behavior of WLI sensor system. Therefore, the procedure to design a high voltage OVT using a WLI sensor system as described must include the selection of a scale factor in such a way that the scanning voltage becomes suitable to be driven and measured by an electronic signal processing system.

4.1 Pockels modulators as high voltage sensor interferometers

Recently, different possibilities for development of Pockels modulators specially designed for direct measurement of high voltages have been investigated. Among these possibilities, a particular approach comprises an unusual configuration of Pockels modulator in which the electro-optic crystal is divided in several slices (Santos et al., 2000). This kind of modulator, which is called multi-segmented Pockels sensor, allows V_π to be defined to arbitrarily high value. Several prototype versions of devices based on such approach were already built and tested, demonstrating their suitability to be applied as primary sensor in high voltage OVTs.

A basic version of high voltage Pockels sensor in longitudinal modulation configuration consists in an arrangement of one piece of electro-optic Pockels crystal inserted between two aluminum electrodes, which are separated and supported by acrylic tubes. In a prototype formerly built, the electro-optic crystal used was a piece of $Bi_3Ge_4O_{12}$ (BGO) in parallelepiped shape (1x5x100 mm) encapsulated in an acrylic cylinder. Since BGO exhibits n_o = 2.098 and r_{41} = 1.03x10^{-12} (m/V), and using a SLD operating in λ = 1.321 μm as light source in the high voltage sensor described, the half-wave voltage calculated using eq. (6) is: $V_\pi \cong$ 69.4 kV.

In order to increase V_π value, a high voltage Pockels sensor using longitudinal modulation in a multi-segmented configuration was developed to be used as sensor interferometer in an OVT prototype (Santos, 1996). Such sensor is composed by electro-optic crystals and pieces of dielectric material acting as mechanical supports that maintain the crystals spaced by gaps, as shown in Fig.4.

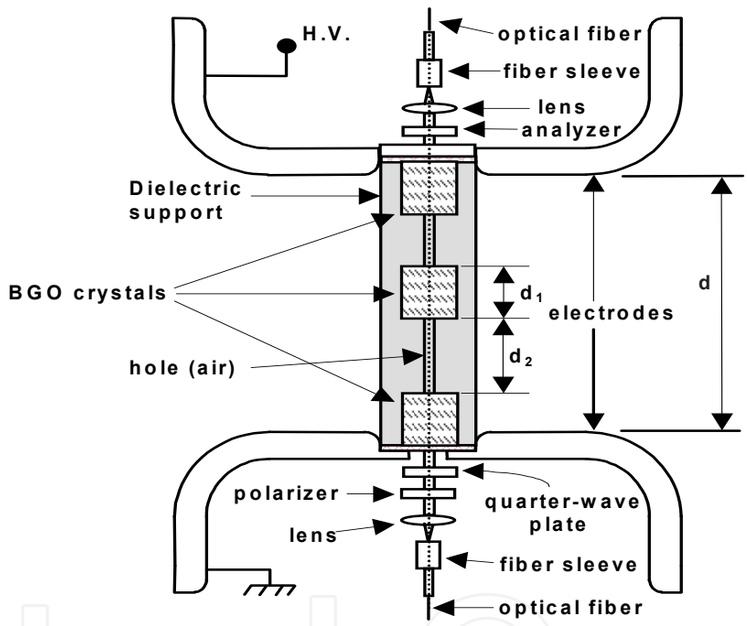

Fig. 4. Multi-segmented high voltage electro-optical sensor.

A simple method to make an estimation of V_π voltage for multi-segmented sensors is achieved by using the expressions (Santos, 1996):

$$V_\pi = \frac{(\lambda . K)}{2 \, . \, n_0^3 \, . \, r_{41} \, n \, . \, d_1} \tag{19}$$

$$K = \left[n \, . \, d_1 + \frac{\varepsilon_1}{\varepsilon_2}(n-1) \, . \, d_2 \right] \tag{20}$$

where n is the number of crystal pieces, d_1 is their thickness, d_2 *is* the thickness of gaps, ε_1 is the permittivity of crystal and ε_2 is the permittivity of gas medium filling the gaps.

Although eq. (20) is a good approximation when crystal pieces are thin (≅ 1 mm), it does not remain valid when the thickness d_1 increases, due to non-uniformities of electric field inside the pieces. An equivalent value of K that allows a better estimation of V_π can be found from the voltage applied to electrodes and the average value of electric field in crystal pieces by:

$$K = \frac{V}{\overline{E}} \tag{21}$$

$$\overline{E} = \frac{1}{n}\sum_{i=1}^{n}\overline{E_i} \tag{22}$$

The average values of electric fields inside the crystals, $\overline{E}_i$, were computed by applying a 2D multiphysics simulation software based on finite elements method (FEM), which allows the exploration of axial symmetry presented by the sensor (Rubini et al., 2004). This kind of software has been used in analysis by FEM simulation of several electro-optic components, including integrated optics devices (Franco et al., 1999).

For example, using 3 pieces of BGO having d_1 = 6,26 mm, placed in a sensor as shown in Fig. 4, the calculated value using FEM simulation is: $V_\pi \cong$ 421,9 kV. The experimentally measured value, using a prototype built with same configuration and materials above described, was: $V_\pi \cong$ 439,6 kV. The good agreement between calculated and measured V_π values indicates that multi-segmented approach is suitable for obtaining Pockels modulators appropriate for direct measurement of high voltages.

4.2 Recovery interferometer

In order to allow the identification of the central fringe, a Pockels modulator suitable to be used as recovery interferometer in a WLI sensor system must to be able to reconstruct a significant part of the fringe pattern. Since each fringe is within an interval of 2π radians of phase difference and V_π is the voltage necessary to produce π radians of phase difference in a Pockels modulator, it follows that a Pockels recovery interferometer must have V_π as small as possible. Even though in a particular WLI sensor system multi fringe recovering is not required, a small V_π value is favorable for the electronic signal processing system, which is responsible for driving the scanning voltage V_r.

Reduction of V_π in electro-optic modulators can be achieved, for example, by adopting a transverse modulation configuration. In this case, the relation between electric field and applied voltage is given by $E = V/d$, and, from eq. (4) and eq. (5), V_π becomes:

$$V_\pi = \frac{\lambda}{2n_o^3 r_{41}}\frac{d}{L} \tag{23}$$

To achieve smaller values of V_π, the ratio d/L must be minimized. Using a piece of BGO, in parallelepiped shape with dimensions of d = 1 mm and L = 100 mm, as electro-optic crystal in a prototype of recovery interferometer, and the same light source described before, the half-wave voltage calculated using Eq. (23) is $V_\pi \cong$ 694 V. Although such value can be considered satisfactory for some applications, it is still relatively high.

An alternative to reduce $V_{\pi r}$ even more, as mentioned before, is to make use of materials with a product $n_{or}^3 r_{41r}$ greater than the product $n_{os}^3 r_{41s}$ of crystal used in sensor interferometer. It is possible to find crystals like Barium Strontium Niobate (BSN) that presents Pockels coefficients many times greater than that of BGO, which may allow obtaining much smaller $V_{\pi r}$, as is desirable. Another possibility to obtain electro-optical modulators with low $V_{\pi r}$ is using integrated optical devices, which typically show half-wave voltages around 5 V. However, since there are no integrated optical devices suitable for WLI applications commercially available, development efforts must be done to make feasible this possibility.

5. Signal processing techniques applied to WLI high voltage sensor system

As stated earlier, behavior and performance characteristics of a WLI sensor system, as dynamic range, accuracy, resolution, bandwidth, thermal stability, etc., are all dependent on the association of an encoding technique with a signal processing technique.

The presented encoding technique based on Pockels modulators linked by optical fibers may, potentially, allow a WLI sensor system applied as OVT to have large bandwidth, high accuracy and fine resolution, among other desirable characteristics. However, since Pockels modulators can be seen as polarimetric interferometers, high voltages measured are traduced in terms of optical intensity at their outputs. Therefore, the measurement becomes dependent on link losses, which can change unpredictably in time.

Recently, applications of specially designed electronic signal processing systems have been proposed as options to overcome such problem (Almeida, 2001; Santos, 1996). The main idea behind these signal processing techniques is to take advantage of a particular property arising in WLI sensor systems when fixed OPDs introduced by compensation plates are larger than coherence length of the light source. In this case, from eq. (12) it is possible to observe that, since visibility approaches to zero, the information in the output of sensor interferometer is encoded only in the spectrum of light, suggesting that a measurement can be done independently of optical intensity present in the optical fiber link output.

In WLI systems using sensor and recovery interferometers connected in series, both introducing identical fixed OPDs, the information is translated back to the amplitude domain, as shown by eq. (13), and measuring can be done in a large bandwidth, but becomes again dependent on the optical intensity at output of system. To achieve a WLI sensor system that provides measurements independent on optical intensity it is necessary to develop electronic signal processing techniques specially designed to compensate optical intensity fluctuations not related to the measurand.

Following, two topologies of WLI sensor systems, using different encoding techniques associated with their specific signal processing techniques, both able to offer a.c. high voltage measurements compensated for optical intensity fluctuations, are presented. Prototypes were built and tested, and experimental results are presented and commented.

5.1 Peak and valleys values detection technique

5.1.1 Principle of operation

The strategy adopted in this signal processor approach is based on the precise detection of peaks and valleys values present in the output signal of a modulated recovery

interferometer, which contains desired information about the ac high-voltage applied to the specially designed Pockels modulator used as sensor interferometer.

The analysis of this patent pending signal processing technique may start by the photo-current, $I_d(t)$, detected at output of optical fiber emerging from recovery interferometer, which is proportional to optical intensity, $I(t)$, as shown in Fig.5 (Almeida & Filho, 2003).

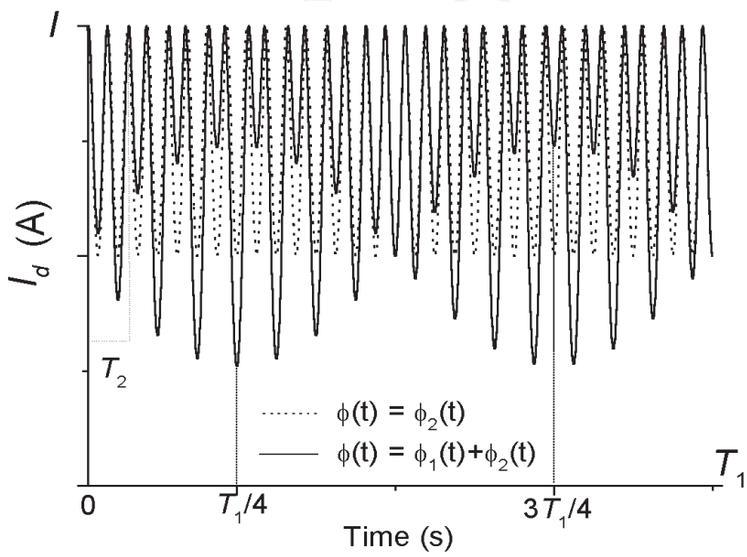

Fig. 5. Photo-current, I_d (t), for a period T_1 of the phase of modulation voltage applied to the sensor interferometer.

The behavior of $I_d(t)$ is shown in Fig. 5 for a particular condition, characterized by the phases of modulating voltages $\varphi_1(t) = \varphi_1 \sin\omega_1 t$ and $\varphi_2(t) = \varphi_2 \sin\omega_2 t$, applied, respectively, to sensor and recovery interferometers. To better explain the principle of operation, it were adopted $\omega_2 = 16\omega_1$, $\varphi_1(t) = 0{,}5$ radian, $\varphi_2(t) = \pi/2$ radians. $T_1 = 1/f_1$ is the period of fundamental frequency f_1 of $\varphi_1(t)$ and $\omega_2 = 1/T_2$ ($T_2 = T_1/16$).

In Fig. 5 it is illustrated that:

- the valley values change with the presence of phase modulation $\varphi_1(t)$ due to the ac high voltage applied to the sensor interferometer,
- these changes occur at the instants $T_2/4$ and $3T_2/4$ of each cycle of phase modulation $\varphi_2(t)$ applied to the recovery interferometer. This deviation of valley values occurs alternately bellow and above the reference value obtained without the phase modulation, $\varphi_1(t)$,
- the peak values don't change with the presence of phase modulation $\varphi_1(t)$ due to the ac high-voltage applied to the sensor interferometer. However, their positions change and occur symmetrically to the instant $T_2/2$ at each cycle of phase modulation, $\varphi_2(t)$.

In order to clarify the topics above, in Fig.6 it is shown a zoom in time, detailing one cycle of the voltage $V_d(t)$, present at the output of a transimpedance amplifier, used to convert the photocurrent $I_d(t)$ to voltage. An ideal transimpedance amplifier built in a classical configuration presents an output voltage $V(t)$ given by:

$$V(t) = R_f\, I(t) \tag{24}$$

were R_f is the feedback resistance, which is numerically equal to the transimpedance gain, G.

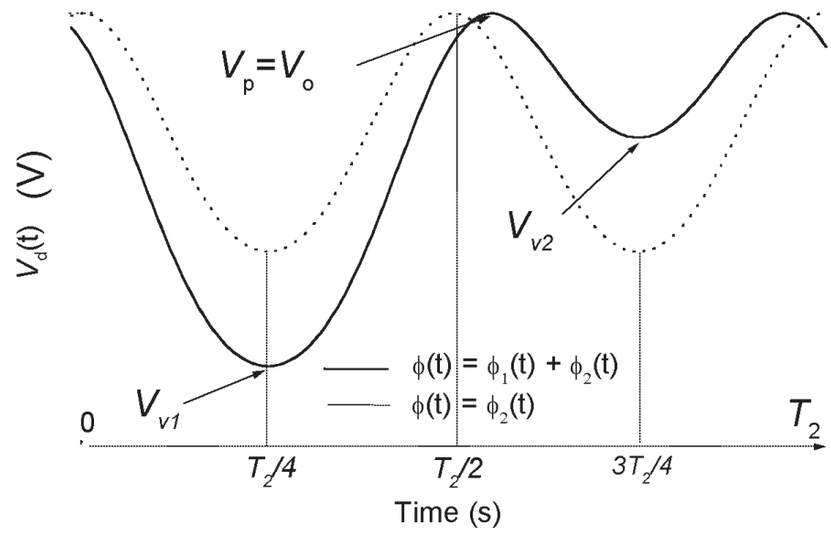

Fig. 6. Magnification in time showing output voltage at the output of transimpedance amplifier in a period of T_2.

In Fig.6 it is shown the occurrence of:

- a valley value V_{v1} and a valley value V_{v2}, bellow and above, respectively, reference value, represented by the dotted line, obtained for $\varphi_1(t)$ = 0 radian,
- a peak value occurring after $T_2/2$.

The photo current, can be expressed by (Santos et al., 2002):

$$I_d(t) = \frac{I_o}{2}\left\{1 + \cos\left[\varphi_1(t) + \varphi_2 \sin\omega_2 t\right]\right\} \tag{25}$$

where I_o is its maximum value. $I_d(t)$ can also be expressed using Bessel functions as:

$$\begin{aligned} I_d(t) = I_o\left\{1 + \frac{1}{2}\left[J_0(\varphi_2) + 2\sum_n J_{2n}(\varphi_2)\cos(2n\omega_2 t)\right]\cos\left[\varphi_1(t)\right]\right\} + \\ - I_o\left\{\sum_n J_{2n-1}(\varphi_2)\sin\left[(2n-1)\omega_2 t\right]\sin\left[\varphi_1(t)\right]\right\} \end{aligned} \tag{26}$$

where $n \in N^*$, and J_n denotes the nth order Bessel function of first kind (Almeida, 2001).

From eq. (25) and eq. (26) it is obtained the expression for the low frequency components of $I_d(t)$, labeled as $I_{lf}(t)$ and characterized by $\omega \langle\langle \omega_2 - \omega_1$, as:

$$I_{lf}(t) = I_o\left\{1 + \frac{1}{2}J_0(\varphi_2)\cos\left[\varphi_1(t)\right]\right\} \tag{27}$$

Likewise, from eq. (24) and eq. (27) the low frequency components of $V_d(t)$, termed as $V_{lf}(t)$, can be expressed as:

$$V_{lf}(t) = V_o\left\{1 + \frac{1}{2}J_0(\varphi_2)\cos\left[\varphi_1(t)\right]\right\} \tag{28}$$

Based on eq. (24) and eq. (26) the high frequency components of $V_d(t)$ labeled as $V_{hf}(t)$ and identified by $\omega_2 - \omega_1 \rangle\rangle \omega_1$ can be written as:

$$V_{hf}(t) = V_o\left(\frac{1}{2}\left\{\cos\left[\varphi_1(t) + \varphi_2 \sin\omega t\right] - J_0(\varphi_2)\cos\left[\varphi_1(t)\right]\right\}\right) \tag{29}$$

From eq. (29) results that, the valley values of $V_{hf}(t)$, from now on termed $V_{v1}(t)$ and $V_{v2}(t)$, can be expressed in each cycle of $\varphi_2(t)$ as:

$$V_{v1} = \frac{V_o}{2}\left\{\cos\left[\varphi_2 + \varphi_1(t)\right] - J_0(\varphi_2)\cos\left[\varphi_1(t)\right]\right\} \tag{30}$$

$$V_{v2} = \frac{V_o}{2}\left\{\cos\left[\varphi_2 - \varphi_1(t)\right] - J_0(\varphi_2)\cos\left[\varphi_1(t)\right]\right\} \tag{31}$$

A straightforward substitution of trigonometric identities in eq. (30) and eq. (31), gives:

$$V_{v1}(t) = \frac{V_o}{2}\left\{\cos\varphi_2\cos\left[\varphi_1(t)\right] - \sin\varphi_2\sin\left[\varphi_1(t)\right]\right\} - \frac{V_o}{2}\left\{J_0(\varphi_2)\cos\left[\varphi_1(t)\right]\right\} \tag{32}$$

$$V_{v2}(t) = \frac{V_o}{2}\left\{\cos\varphi_2\cos\left[\varphi_1(t)\right] + \sin\varphi_2\sin\left[\varphi_1(t)\right]\right\} - \frac{V_o}{2}\left\{J_0(\varphi_2)\cos\left[\varphi_1(t)\right]\right\} \tag{33}$$

In order to maximize the influence of $\varphi_1(t)$ in the difference between $V_{v1}(t)$ and $V_{v2}(t)$, one should set $\varphi_2 = \pi/2$ radians as peak value of phase modulation $\varphi_2(t)$. Such a substitution in eq. (32) and eq. (33) results in:

$$V_{v1}(t) = \frac{V_o}{2}\left\{-\sin\left[\varphi_1(t)\right] - J_o(\pi/2)\cos\left[\varphi_1(t)\right]\right\} \tag{34}$$

$$V_{v2}(t) = \frac{V_o}{2}\left\{\sin\left[\varphi_1(t)\right] - J_o(\pi/2)\cos\left[\varphi_1(t)\right]\right\} \tag{35}$$

From eq. (34) and eq. (35), $\varphi_1(t)$ can be written as:

$$\varphi_1(t) = \arcsin\left[\frac{V_{v2}(t) - V_{v1}(t)}{(V_o / 1{,}5)}\right] \tag{36}$$

Strictly speaking, the parameter V_o changes with fluctuations in the intensity of the light incident on the photodiode and should be written as $V_o(t)$. In spite of that, eq. (36) shows that, from a theoretical point of view, these fluctuations have no influence on the measured

value of $\varphi_1(t)$. From (36), in the interval $0 \leq \varphi_2 \leq \pi$, $\varphi_2 = \pi/2$ radians is the peak value of the phase modulation, $\varphi_2(t)$, which:

- maximizes the differential sensitivity between the valley values $V_{v1}(t)$ and $V_{v2}(t)$ as regard to $\varphi_1(t)$;
- minimizes the dependence of scale factor with respect to time fluctuations in φ_2, since that $\partial\varphi_2(t)/\partial t = 0$ for this point of operation;
- maximizes the dynamic range for the measurement of $\varphi_1(t)$, i.e., $|\varphi_1(t)|_{\max} = \pi/2$ radians.

The presented technique allows keeping control of phase modulation depth, φ_2, by means of:

$$\varphi_2 = \arcsin\left[\frac{V_{v2}(t) + V_{v1}(t)}{(V_o / 1{,}5)}\right] \tag{37}$$

likewise as provided by other techniques proposed for processing interferometric signals, based on division of RMS values of some of its harmonics or zero-crossings (Burns, 1994; Tselikov et al., 1998).

A blocks diagram of electronic signal processor developed for demodulating ac high voltages applied to OVT prototype is shown in Fig.7.

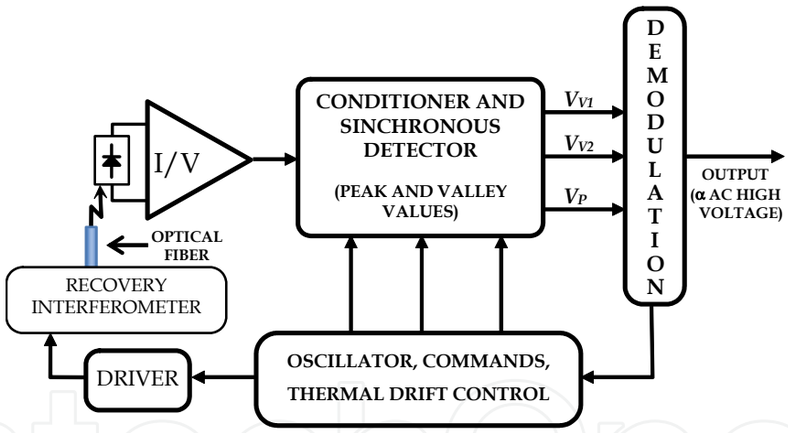

Fig. 7. Blocks diagram of the signal processor applied to the OPT.

The synchronous detection of consecutive peak and valleys values the transimpedance amplifier output yields, according to eq. (37), the demodulation of ac high voltage applied to WLI high voltage sensor system.

5.1.2 Experimental results

Aiming the development of a highly precise OVT based on WLI technique, a prototype of optical fiber sensor system using a Pockels modulator as recovery interferometer was built (Rubini et al., 2004), as shown in Fig. 8.

The sensor system was integrated to the electronic signal processor and the whole set was subjected to ac high-voltage tests conducted to determine the overall performance with

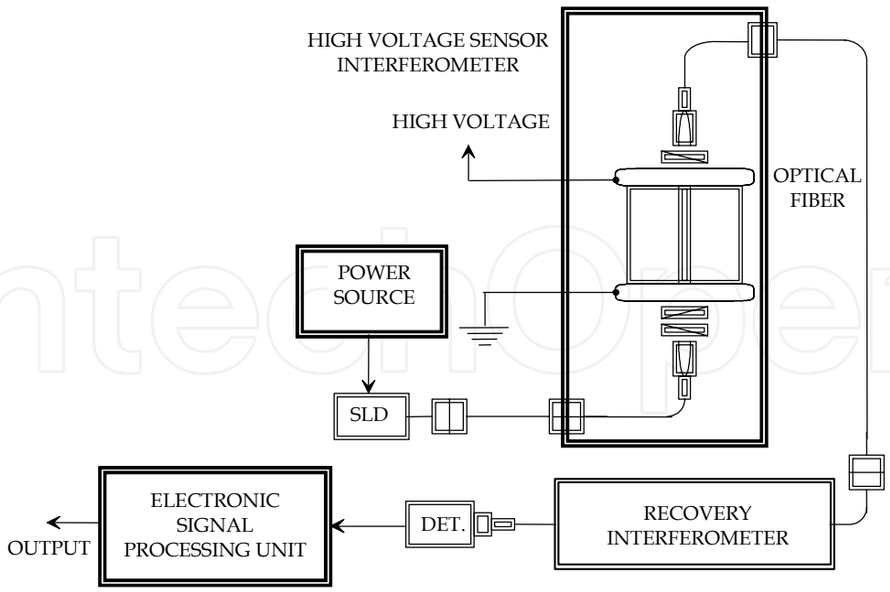

Fig. 8. Blocks diagram of OVT prototype using WLI configuration.

respect to the voltages applied. In Fig.9(a) it is illustrated the OVT used for the essays up to 10 kV_{RMS} applied to the sensor at the Optical Sensors Laboratory (LSO) of University of São Paulo (USP). The sensor interferometer is connected to a conventional instrument voltage transformer, rated 80.5 kV primary, 115/230V secondary, 7.5 kVA. Fig. 9(b) illustrates the OVT prototype at

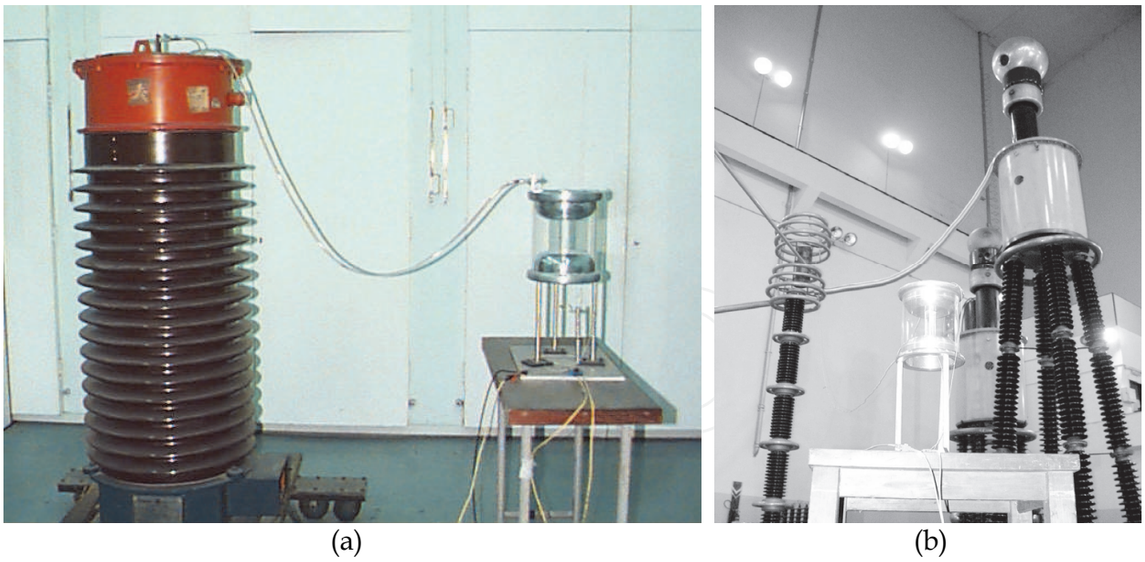

(a) (b)

Fig. 9. Sensor interferometer of the OVT prototype: (a) connected to the voltage transformer at Optical Sensors Laboratory (LSO-USP) and (b) connected to the cascade transformer at High Voltages Laboratory (LAT-IEE/USP).

the High Voltages Laboratory (LAT) facilities of Electrotechnical and Energy Institute (IEE/USP) used for the essays from 10 kV_{RMS} up to 100 kV_{RMS}. The sensor interferometer connected to a high voltage cascade transformer, rated 1000 kV secondary, 150 kVA.

High-voltages at power frequency (60 Hz) up to 80 kV_{RMS} were applied to the sensor interferometer. The experimental results from these tests and related linear regression curve are shown in Fig. 10.

From results shown in Fig. 10, it is observed that a linearity better them +/- 1,5% is obtained.

In addition, from other tests, it was possible to observe good temperature and time stabilities showed by the OVT, lower than 1000 ppm/^{o}C in an observation period of half an hour.

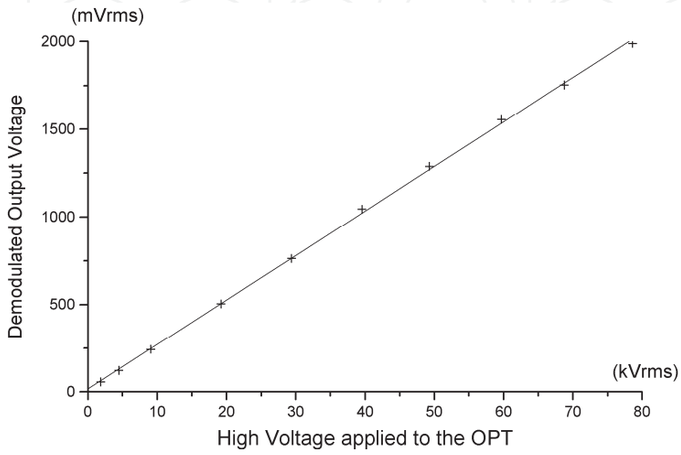

Fig. 10. Demodulated output voltage vs. ac input voltage applied to the sensor interferometer.

Such behaviors are due to the optical encoding technique as well as to the peculiar design of the electronic signal processing technique, which was specially developed for this application. The demodulation bandwidth of 1 kHz used makes possible to efficiently demodulate the firsts 16 harmonics of ac voltage applied to the sensor.

In Fig. 11 it is shown time-domain waveforms of demodulated output voltage and applied voltage (obtained from a reference divider) when about 70 kV_{RMS} is applied to the OVT prototype.

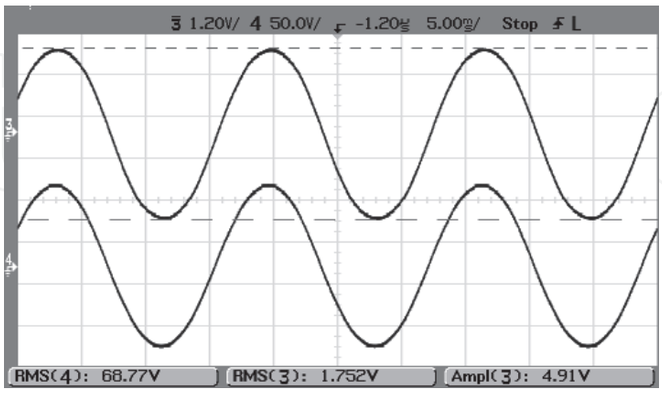

Fig. 11. Waveforms and RMS values of both the output demodulated voltage (channel 3) and ac high voltage applied to the sensor interferometer (channel 4).

In Fig. 12 frequency domain analyses are presented for both the output demodulated voltage and the ac high voltage applied to the sensor interferometer presented in Fig. 11.

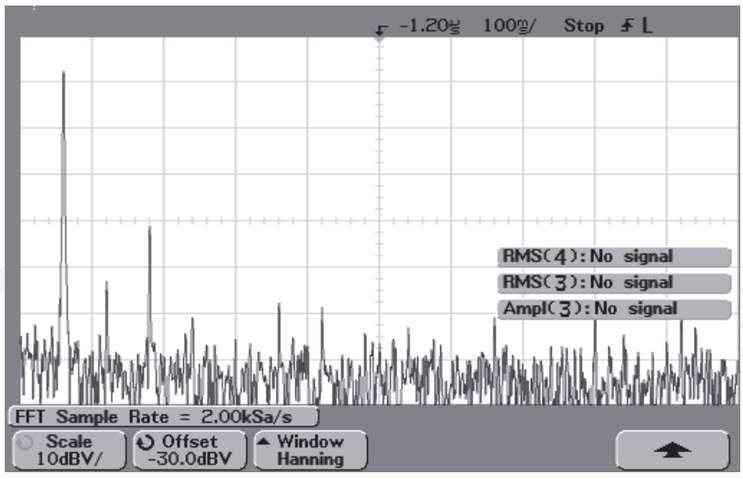

(a)

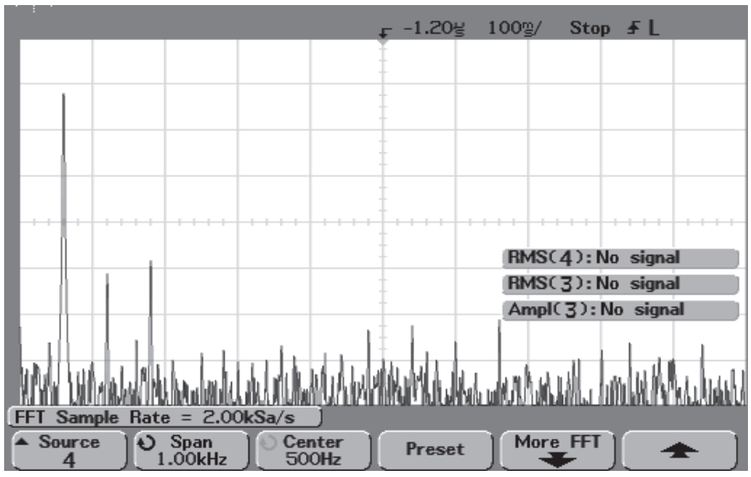

(b)

Fig. 12. Fast Fourier transforms, in the range from 0 kHz to 1 kHz: (a) of output demodulated voltage and (b) of ac high voltage applied to sensor interferometer

Unfortunately, for 70 kV_{RMS} applied to the sensor, the correspondent frequency domain analysis observed in Fig.12(b) can't be extended for frequencies higher than 300 Hz due to the bandwidth limitation of the reference divider used for measuring the amplitude of ac high voltage applied to the sensor interferometer. In spite of that, a great likeness between this spectrum and the one shown in Fig. 12(a) can be observed up to 300 Hz.

5.2 Normalization by an optical power reference sample technique

5.2.1 Principle of operation

To take advantage of WLI technique in a less expensive configuration capable to reduce the dependency of the OVT output voltage, which carries out the measurement information, $V_{ac}(t)$, on optical intensity fluctuations, an alternative encoding technique using an unmodulated recover interferometer was proposed (Santos et al., 2003), as shown in Fig. 13.

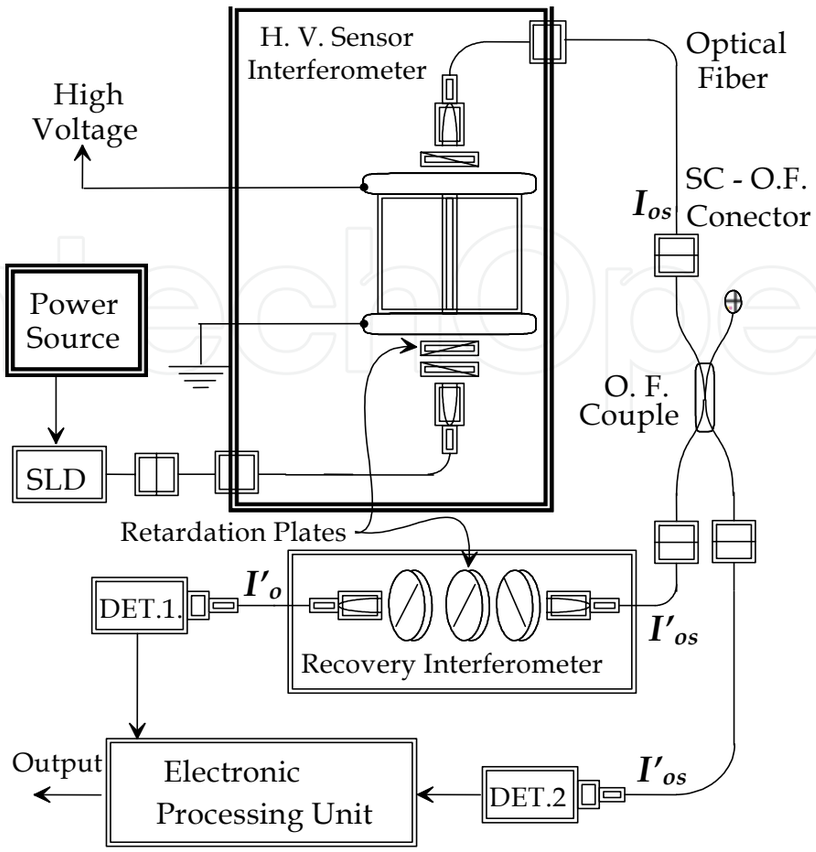

Fig. 13. OVT using WLI sensor system configuration with unmodulated recovery interferometer.

In this system, for recovering the interferometric signal a simple recovery interferometer, composed of a compensation plate inserted between two aligned polarizers, is placed in series with the optical fiber in the return path of sensing system by means of a directional coupler, which is an optical fiber beam splitter. From eq. (12), the optical intensity at the output of the recovery interferometer, I_o, is given by (Santos, 1996):

$$I_o = \frac{1}{4}\alpha_S \alpha_R T_1 T_2 I_i \left\{ 1 + \frac{1}{2} e^{-(\pi \Delta L / L_c)^2} \cos 2\pi \frac{\Delta L}{\lambda_0} \right\} \tag{38}$$

where I_i is the optical power at the input of the system (output of the SLD light source), α_S is the attenuation of light from the SLD to the input of sensor interferometer, λ_0 is the central wavelength of the light source and ΔL is the total OPD in the sensor system, given by: $\Delta L = \Delta L_s - \Delta L_c$.

The compensation plate used in the recovery interferometer is identical to the one used in the sensor interferometer. However, it is mounted in a special positioner, which can rotate around two axes to allow a fine tuning of the OPD introduced. Using this two axes rotation capability, it is possible to set the OPD of recovery interferometer in such way that: $\Delta L_{cr} = \Delta L_{cs} - \lambda_0/4$. In such condition, from eq. (38), I_o becomes:

$$I_o = \frac{1}{4}\alpha_S \alpha_R T_1 T_2 I_i \left\{ 1 + \frac{1}{2} e^{-\left[\frac{\lambda_0}{2} \left(\pi \frac{V}{V_\pi} - \frac{\pi}{2} \right) \Big/ L_c \right]^2} \cos\left(\pi \frac{V}{V_\pi} - \frac{\pi}{2} \right) \right\} \tag{39}$$

Since in practical applications L_c is much larger than λ_0, the exponential term in (39) remains close to the unity when $|V| < V_\pi$. Therefore, I_o can be approximated by:

$$I_o = \bar{I_o} \left(1 + \frac{1}{2} \sin \pi \frac{V}{V_\pi} \right) \tag{40}$$

where $\bar{I_o} = \frac{1}{4}\alpha_S \alpha_R T_1 T_2 I_i = \frac{1}{4}\alpha_t I_i$, is the average of output light intensity.

The response curve for this kind of WLI sensor system is similar to the response curve of a simple polarimetric Pockels modulator and, in this case, also there is a dependency of output light intensity, I_o, on the total attenuation of system. To take advantage of WLI technique and eliminate such dependency, an electronic signal processing scheme was developed, using as reference a sample of light intensity at output of sensor interferometer, I_{os}, which is given by:

$$I_{os} = \frac{1}{2}\alpha_s T_1 T_2 I_i \left\{ 1 + e^{-(\pi \Delta L_s / L_c)^2} \cos 2\pi \frac{\Delta L_s}{\lambda_0} \right\} \tag{41}$$

Since $\Delta L_s >> L_c$, the exponential term in eq. (40) approaches to zero. Therefore, I_{os} reduces to:

$$I_{os} = \frac{1}{2}\alpha_s T_1 T_2 I_i = \frac{2}{\alpha_R} \bar{I_o} \tag{42}$$

As can be seem in Fig. 13, placing a directional coupler between the output of sensor interferometer and the input of recover interferometer it is possible to obtain the signal I'_{os}(t), which is detected by the photodetector (DET. 2) and used to compensate the signal obtained in the output of recover interferometer, I'_o, for any optical power variation. Using a 3 dB directional coupler, the incoming optical intensity is divided in equal parts between the two outputs. Therefore, the optical power I'_{os}, which reaches the photodetector (DET. 2), is:

$$I'_{os} = \alpha_{ex} I_{os} / 2 \tag{43}$$

where α_{ex} is the excess loss of directional coupler and I_{os} is the optical intensity at output of sensor interferometer.

The optical intensity at output of recovery interferometer, I'_o(t), is given by:

$$I'_o(t) = \frac{1}{2}\alpha_r I'_{os} \left(1 + \frac{1}{2} \sin \pi \frac{V_{ac}(t)}{V_\pi} \right) \tag{44}$$

where α_r is the total attenuation of recovery interferometer, I'_{os} is the optical power at output of optical fiber coupler and V_π is the half-wave voltage of sensor interferometer.

A blocks diagram of electronic signal processing unit required by such system is given in Fig. 14.

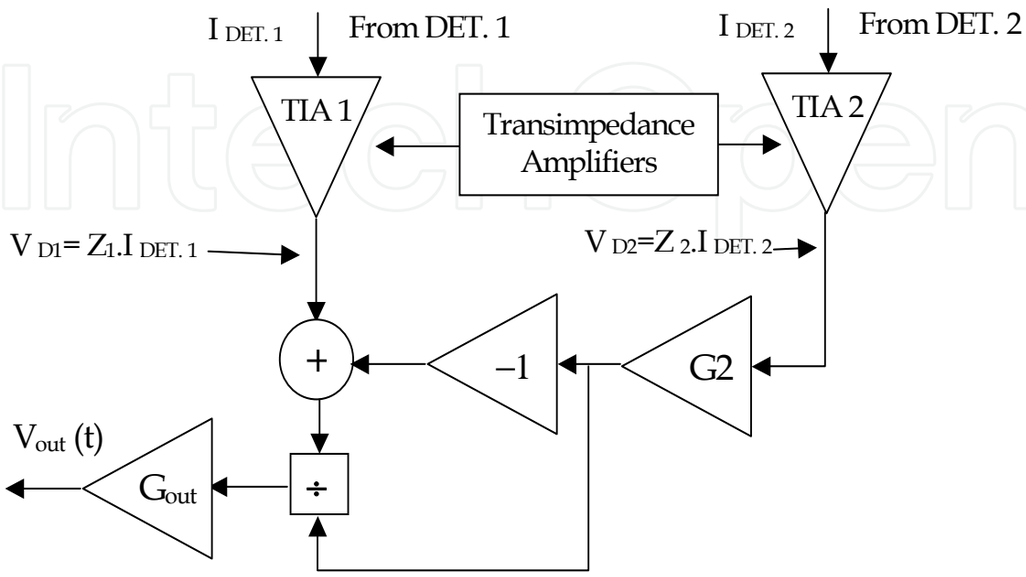

Fig. 14. Blocks diagram of electronic signal processing unit.

Applying the signals I'_{os} and I'_{o}(t) to the electronic signal processing unit proposed in Fig. 14, if the transimpedance gains Z_1 and Z_2 are equals and the gain $G_2 = \alpha_r/2$, the output signal, V_{out}(t), can be linearized (when $V_{ac}(t) << V_{\pi}$) and approximated by the following expression:

$$V_{out}(t) \cong \frac{G_{out}}{2} \cdot \pi \cdot \frac{V_{ac}(t)}{V_{\pi}} \tag{45}$$

where G_{out} is the gain of last amplifier stage.

From eq. (45) it is clear that $V_{out}(t)$ is independent on the optical intensity at optical fiber link, as desired.

5.2.2 Experimental results

To verify the V_{out} dependency on optical power I_{os}, an experimental setup implementing the system described in Fig. 13 was built using prototypes of high voltage Pockels cell and recovery interferometer previously developed (Santos et al., 2000, 2003), a 3 dB directional coupler (commercially available), a SLD operating in a wavelength of 1.3 μm as broadband light source and an electronic signal processing unit developed according to the blocks diagram shown in Fig. 14. To introduce variations in I_{os}, an adjustable optical attenuator was inserted between the output of sensor interferometer and the input of directional coupler.

Experiments were conducted changing the attenuation imposed by the adjustable attenuator in a range of 0 to –8.66 dB. During the variation of the attenuation the voltage applied to the OVT was maintained constant in a reference value of 4.5 kV_{pp}. In Table 2, bellow, the attenuation values introduced by the attenuator, the RMS values of measured signals in the electronic processing unit output and the relative variations of correspondent V_{out} value, named ΔV_{out}, are shown.

Attenuation (dB)	V_{out} **(mV_{RMS})**	ΔV_{out} **(%)**
0	131,9	0
-2,5	131,0	-0,7
-3,46	131,0	-0,7
-4,75	131,1	-0,6
-5,54	132,0	0,1
-6,51	132,0	0,1
-7,49	133,2	1,0
-8,66	133,0	0,8

Table 2. Attenuation values introduced by the attenuator, RMS values of measured signals in the electronic processing unit output and relative variations of the V_{out} values (ΔV_{out}).

From values presented in table 2, it is shown that, for a variation of about -9 dB in average optical power carried by the optical fiber link, less than 1% of variation is observed in output of WLI sensor system.

6. Conclusions

Both alternatives of WLI based OVTs presented have adequate performances for measuring ac high voltages while keeping low sensibility to fluctuations on average light intensity in the optical fiber link.

The advantages exhibited by the first approach, compared to the second one, are the better characteristics in terms of resolution and thermal and temporal stabilities. However, the cost and complexity of that kind of solution are higher than the second one. Such characteristics make first solution suitable for applications where high performance is demanded.

The main advantages of the second approach are the lower cost and smaller complexity of the entire system. Therefore, it is recommended for applications demanding moderate performances and lower prices.

New optical encoding techniques and electronic signal processing techniques applied to WLI sensor systems are still in development, and it is expected that many improvements arise in this field in a near future.

7. Acknowledgment

The authors would like to thank to the University of São Paulo – USP - and to São Paulo Research Foundation - FAPESP - for the financial support to this work.

8. References

Almeida, J. C. J. de & Filho, O. V. A. (2003). *Demodulador de desvio de fase óptico não recíproco num sensor óptico interferométrico, via detecção dos valores dos picos da corrente detectada no fotodetector acoplado à saída do interferômetro óptico*, patent required to the Instituto Nacional da Propriedade Industrial - INPI, according to the registry number PI0303.688-0, Brazil

Almeida, J. C. J. de, (2001). *Nova Técnica de Processamento de Sinal no Domínio do Tempo de Giroscópios Interferométricos de Sagnac a Fibra Óptica*, Ph.D. Thesis, State University of Campinas, Brazil

Bull, J. D., Jaeger, N. A. F., & Rahmatian, F. (2005). A new hybrid current sensor for high-voltage applications. IEEE Transactions on Power Delivery, Vol. 20, No. 1, (Jan 2005), pp. 32-38, ISSN 0885-8977.

Burns, W. K. (1994). *Optical Fiber Rotation Sensing*, (Ed. 1), Academic Press, Inc., ISBN 0-1214.6075-4, Boston, USA

Chen, S.; Palmer, A. W.; Grattan, K. T. V.; & Meggit, B. T. (1992). Digital signal-processing techniques for electronically scanned optical-fiber white-light interferometry, *Applied Optics*, Vol. 31, No. 28, (October 1992), pp. 6003-6010, ISSN 1559-128X

Chen, X.; Ye, W.; Zhang, H. & Liu, T. (2010). Spectral domain demodulation of fibre optics position and displacement sensors by Fourier-transform spectral interferogram. *Proceedings of 9th International Conference on Optical Communications and Networks (ICOCN 2010)*, ISBN 978-1-84919-314-6, Nanjing, China, October 2010.

Crotti , G.; Sardi, A.; Kuljaca, N.; Mazza, P.; De Donà, G.; Brand, U.; Giraud, M.; A. Andersson & Weiss, S. (2006). "On-site live verification of HV instrument transformer accuracy", CIGRE General Session 41, Aug. 27 - Sep. 1, 2006, paper A3-204

Franco, M. A. R.; Passaro, A.; Sircilli, F. & Cardoso, J. R. (1999). Finite element analysis of anisotropic optical waveguide with arbitrary index profile. *IEEE Transactions on Magnetics*, Vol.35, No. 3, (May 1999), pp. 1546-1549, ISSN 0018-9464

Françon, M. (1967). *Optical Interferometry*, Academic Press, ISBN 0-1226.6350-0, New York, USA

Kim, J.H. (2008). An All Fiber White Light Interferometric Absolute Temperature Measurement System. Sensors, 8, 6825-6845. ISSN 1424-8220

Lequine, M.; Lecot, C.; Giovannini, H.; & Huard, S. (1990). A dual wavelegth passive homodyne detection unit for fiber coupled white light interferometers, In: *Fiber-Optic Sensors IV*, Vol. 1267, Editor: Ralf T. Kersten, pp. 288-293, Proceedings of SPIE, ISBN 9780819403148

Liao, H. & Yang, Y. (2010). A Linnik Scanning White-Light Interferometry System Using a MEMS Digital-to-Analog Converter, Proc. Eurosensors XXIV, September 5-8, 2010, Linz, Austria Volume 5, 2010, Pages 758-761, ISSN: 1877-7058.

Mariscotti, A. (2009). A Rogowski winding with high voltage immunity, In: EUROCON 2009 pp. 1129-1133, ISBN 978-1-4244-3860-0, St. Petersburg, RU, May 18-23 2009.

Murtaza, G. (1991). *Dual Wavelength referenced intensity modulated optical fibre sensor system*, PhD Thesys, Manchester Polytechnic, CNAA

Ning, Y. N.; Grattan, K. T. V.; & Palmer, A.W. (1995). In: *Applications of Photonic Technology*, Editors: Lampropoulos, G. A.; Chrostowsky, J. & Measures, R. M., pp. 339-342, Plenum Press, ISBN 0-3064.5011-9

Rahmatian, F. (2010). High-voltage current and voltage sensors for a smarter transmission grid and their use in live-line testing and calibration, In: *IEEE Power and Energy Society General Meeting*, Minneapolis, MN, ISSN: 1944-9925, E-ISBN: 978-1-4244-8357-0, Print ISBN: 978-1-4244-6549-1, July 2010

Rubini Jr., J.; A. Passaro, Abe, N. M. & Santos, J. C. (2004) Analysis of the electric field distribution in an electrooptic sensor for pulsed high-voltage measurements, *Proceedings of Fifth IEE International Conference on Computation in Electromagnetics – CEM2004*, pp. 71-72, ISBN 0-8634.1400-1, Stratford-upon-Avon, UK, April 19-22, 2004

Santos, J. C. (2009). Contribuições para o desenvolvimento de transformadores de potencial a fibras ópticas (TPs Ópticos) aplicáveis em sistemas elétricos de potência, L.D. Thesis, University of São Paulo, Brazil.

Santos, J. C.; Côrtes, A. L. & Hidaka, K. (1999). A New Electro-optical Method for recovering White Light Interferometric Signals, *Proceedings of 1999 International Microwave And Optoeletronics Conference - IMOC´99*, ISBN 0-7803-5807-4, Rio de Janeiro, Brazil, August 1999

Santos, J. C.; Côrtes, A. L.; Hidaka, K. & Silva, L. P. C. (2003). Improved optical sensor for high voltage measurement using white light interferometry, *Proceedings of SBMO/IEEE MTT-S IMOC 2003*, ISBN 0-7803-7824-5, Fóz do Iguacú, Paraná, Brazil, September 2003

Santos, J.C.; Hidaka, K. & Côrtes, A. L. (2002). Optical High Voltage Measurement Transformer Using White Light Interferometry, *Proceedings of 2002 IEEE/PES T&D Latin America Conference*, in CD-ROM, São Paulo, Brazil, March 2002

Santos, J.C.; Taplamacioglu, M. C. & Hidaka, K. (2000) Pockels high-voltage measurement system. *IEEE Transactions on Power Delivery*, Vol.15, No.1, (January 2000), pp. 8–13, ISSN 0885-8977

Tselikov, A.; Arruda, J. U. & Blake, J. (1998). Zero-Crossing Demodulation for Open Loop Sagnac Interferometers, *IEEE Journal of Lightwave Technology*, Vol. 16, No. 9, (September 1998), pp. 1613-1619, ISSN 0733-8724

Velosa, J.; Gouveia, C.; Frazao, O.; Jorge, P. & Baptista, J. (2011). Digital Control of a White Light System for Optical Fiber Interferometers. *IEEE Sensors Journal*, Vol. PP, No. 99, (April 2011), pp. 1 – 1, ISSN: 1530-437X

Yariv, A. & Yeh, P. (1984). *Optical waves in cristals*. (Ed. 1), Wiley-Interscience, ISBN 0-4714.3081-1, New York, USA

Yu, B.; A. Wang, Gary Pickrell & Xu, J. (2005) "Tunable-optical-filter-based white-light interferometry for sensing," Opt. Lett. 30, 1452-1454 (2005), Optics Letters, Vol. 30, Issue 12, pp. 1452-1454, ISSN: 0146-9592

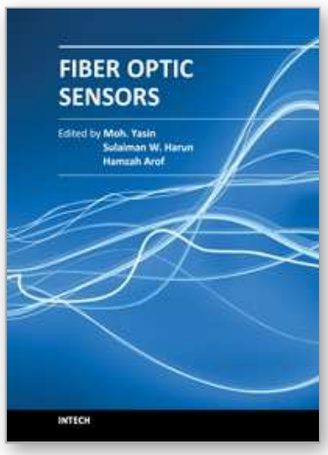

Fiber Optic Sensors
Edited by Dr Moh. Yasin

ISBN 978-953-307-922-6
Hard cover, 518 pages
Publisher InTech
Published online 22, February, 2012
Published in print edition February, 2012

This book presents a comprehensive account of recent advances and researches in fiber optic sensor technology. It consists of 21 chapters encompassing the recent progress in the subject, basic principles of various sensor types, their applications in structural health monitoring and the measurement of various physical, chemical and biological parameters. It also highlights the development of fiber optic sensors, their applications by providing various new methods for sensing and systems, and describing recent developments in fiber Bragg grating, tapered optical fiber, polymer optical fiber, long period fiber grating, reflectometry and interefometry based sensors. Edited by three scientists with a wide knowledge of the field and the community, the book brings together leading academics and practitioners in a comprehensive and incisive treatment of the subject. This is an essential reference for researchers working and teaching in optical fiber sensor technology, and for industrial users who need to be aware of current developments and new areas in optical fiber sensor devices.

InTech Europe
University Campus STeP Ri
Slavka Krautzeka 83/A
51000 Rijeka, Croatia
Phone: +385 (51) 770 447
Fax: +385 (51) 686 166
www.intechopen.com

InTech China
Unit 405, Office Block, Hotel Equatorial Shanghai
No.65, Yan An Road (West), Shanghai, 200040, China
中国上海市延安西路65号上海国际贵都大饭店办公楼405单元
Phone: +86-21-62489820
Fax: +86-21-62489821

IntechOpen